Impact of Spatially Continuous Urban Surface Properties on Heatwave Simulations: A Multi-City Analysis

Timothy Jiang[1], TC Chakraborty[1], Yifan Cheng[2], Rohit Mukherjee[1], Lei Zhao[2], and Alberto Martilli[3]

[1]Pacific Northwest National Laboratory, Richland, WA, USA
[2]University of Illinois, Urbana-Champaign, IL, USA
[3]CIEMAT, Madrid, Spain

This is a non-peer reviewed preprint submitted to EarthArXiv. It has been submitted to the Journal of Advances in Modeling Earth Systems for peer review.

Corresponding author: TC Chakraborty, `tc.chakraborty@pnnl.gov`

Impact of Spatially Continuous Urban Surface Properties on Heatwave Simulations: A Multi-City Analysis

Timothy Jiang[1], TC Chakraborty[1], Yifan Cheng[2], Rohit Mukherjee[1], Lei Zhao[2], and Alberto Martilli[3]

[1]Pacific Northwest National Laboratory, Richland, WA, USA
[2]University of Illinois, Urbana-Champaign, IL, USA
[3]CIEMAT, Madrid, Spain

Key Points:

- U-Surf dataset modified to be structurally consistent with urban canopy scheme of WRF regional climate model
- High-resolution heatwave simulations performed using default parameters and updated U-Surf-WRF for 13 major U.S. cities
- Spatially continuous parameters better capture range of intra-urban variability in temperature, humidity, and heat stress

Corresponding author: TC Chakraborty, tc.chakraborty@pnnl.gov

Abstract

Urban areas are unique in form and function, and representing them in process-based models requires prescribing facet-level morphological and radiative properties, among others. Most urban canopy models prescribe these by density class or local climate zone (LCZ), assigning identical values across broad regions or worldwide. However, properties can vary widely between and within cities. Global km-scale urban facet-level property datasets have recently emerged, but have seldom been applied in regional modeling. Here, we incorporate one such dataset, U-Surf, into the Weather Research and Forecasting (WRF) model, modifying it for WRF's multi-layer urban canopy model and releasing it as U-Surf-WRF. Considering 13 U.S. cities, U-Surf-WRF parameters vary more between LCZs than default WRF parameters, with consistently lower impervious fraction.

To determine the effects of using U-Surf-WRF, we conduct high-resolution (1 km) WRF simulations of recent heatwaves for these 13 cities using default and U-Surf-WRF parameters. Either prescribed by LCZ or for each grid point, using U-Surf-WRF yields more accurate surface temperatures. It also generally decreases modeled urban air temperature and increases modeled urban humidity, yielding lower simulated urban heat and dry islands. Decomposing the impact of each U-Surf-WRF variable, we find that albedo is useful for daytime simulations, especially for air temperature, but that morphology and impervious fraction are most relevant, especially for surface temperature. This study demonstrates the importance of city-specific, facet-level urban properties in urban weather and climate simulations. Conversely, in WRF simulations with poorly constrained parameters, we suggest caution interpreting the magnitude and spatial variability of urban signals.

Plain Language Summary

To simulate near-surface urban weather and climate, models need several urban parameters, for example building height and albedo. Many modeling studies use default parameters, which are often the same for cities throughout the world, mainly due to the unavailability of city-specific estimates. Newly emerging urban data products have worldwide coverage on the km scale but have yet to be widely taken up in practice. Here, we modify one such dataset, U-Surf, for implementation into the Weather Research and Forecasting (WRF) model, naming it U-Surf-WRF. U-Surf-WRF parameters are less urban than WRF defaults for 13 major U.S. cities. We simulate recent heatwaves in these cities using default properties and U-Surf-WRF. U-Surf-WRF simulated urban surface temperatures are closer to observed values, more realistically capturing the range of temperatures across the city. In general, U-Surf-WRF simulations yield higher humidity, lower temperatures, and correspondingly smaller urban heat and dry islands. We break down which U-Surf variables contribute to increased accuracy both when implemented by neighbourhood type (which WRF can do by default) and when prescribed on the km scale, which involves modifying WRF. We find that building height and urban fraction data are most important overall, but that albedo is relevant during the day.

1 Introduction

Growing populations, urban expansion, and background warming have all generally increased the risk posed by urban weather extremes (Liu et al., 2022; Tuholske et al., 2021). Since various physical processes associated with urbanization modify local climate (Qian et al., 2022; Arnfield, 2003), we need urban-resolving models that can represent these processes and capture urban weather and climate signals across spatiotemporal scales (Sharma et al., 2021). Such models are critical for projecting extreme weather in cities and informing mitigation and adaptation strategies (Zhao et al., 2021; Jiang, Krayenhoff, et al., 2025), especially relevant because different urban areas can have unique form and function with distinct, sometimes non-linear, interactions with background weather and climate (Stokes & Seto, 2019; Zhao et al., 2014). Several advances have been made in this regard in the last few decades, including the incorporation of coupled urban canopy models (UCMs) in regional climate models (Hamdi et al., 2012), the development of multi-layer UCMs (Martilli et al., 2002), their integration with building energy schemes (Salamanca et al., 2010), and the addition of vegetation into UCMs (Krayenhoff et al., 2020). There has also been a push to incorporate and advance urban-resolving modeling in global Earth systems models (ESMs) (Oleson & Feddema, 2020).

Not only are distinct urban areas unique in form and function, they also differ greatly from surrounding natural landscapes in terms of radiative, morphological, and thermal properties (Wu et al., 2024; Chakraborty et al., 2021). Thus, these urban-specific parameters are important to better constrain physical processes, such as the surface energy budget, in the urban environment, and to represent interactions between urban areas and their surroundings. However, our ability to constrain these parameters in process-based models is currently simple, partly stemming from a dearth of available data and partly due to model structure (Cheng et al., 2025). Many regional weather and climate models, including the Weather Research & Forecasting (WRF) model, the most used such model for examining urban climate mitigation strategies (Krayenhoff et al., 2021), use coarsely prescribed urban parameters – by region, broad urban class, or both – to capture urban impacts on the surface energy budget and near-surface microclimate. Many such parameters have been estimated for individual cities on an ad hoc basis, mainly focused on regions for which ground data are available, and rarely representing the full range of variability of cities across the world. Moreover, these parameters can often be outdated since urban properties have often evolved over time and in distinct ways across regions (H. Du et al., 2025; Chakraborty & Qian, 2024; Wu et al., 2024).

Ideally, modelers would update prescribed urban parameters to reflect properties for simulation regions and periods. However, such data are often unavailable, especially for multi-city studies over large simulation domains, and so the default parameter values are often used. Data from WUDAPT (Ching et al., 2018) (World Urban Database and Access Portal Tools) have been applied over several cities worldwide, but they often do not cover the entire city and are not available for most cities.

Even within cities, urban parameters are spatially heterogeneous, with relevance for intra-urban variability in climate hazard and exposure (Chakraborty, Newman, et al., 2023). Therefore, this heterogeneity is commonly represented in regional weather and climate models, often in one of the following ways:

1) By representing all urban heterogeneity as various fractions of natural and impervious surfaces (Newman et al., 2024).

2) By capturing modes of variability of urban heterogeneity using three or four density classes, as done in some ESMs (Jackson et al., 2013).

3) The local climate zone (LCZ) framework (Stewart & Oke, 2012), which classifies urban development patterns into ten urban (and seven "natural") categories.

Here, we focus on the LCZ framework as it represents the state-of-the-art standard for urban-resolving regional weather and climate modeling, and can be used relatively simply in recent releases of WRF (Demuzere et al., 2022). LCZs provide around ten modes of variability to represent urban surface properties within the city, while many urban density class schemes provide only three. However, radiative and morphological data by LCZ tailored for individual cities remain scarce. Thus, even within the LCZ framework (Stewart & Oke, 2012), studies often use default urban radiative and morphological parameters for each LCZ. The accuracy of this assumption is questioned, given that these parameters were heuristically derived, and users are cautioned in WRF that "The default values are probably not appropriate for any given city" as well as that "Users should adapt these values based on the city they are working with."

To address the need for city-specific and intra-urban surface constraints, several groups have recently leveraged satellite measurements and derived products to generate global spatially continuous estimates of urban parameters. This includes GLOBUS (GLObal Building heights for Urban Studies) (Kamath et al., 2024), GLAMOUR (Global Building Morphology dataset for URban hydroclimate modelling) (Li et al., 2024), GloUCP: Global urban canopy parameters (Global Urban Canopy Parameters) (Liao et al., 2024), 3D-GloBFP (3-Dimensional Global Building Footprints) (Che et al., 2024), and U-Surf (Cheng et al., 2025). These datasets are derived from various global sources and processed to make them suitable for urban climate modeling.

Most of the datasets above focus on the morphological features of cities. Given their recent development, few studies to date have applied these products, although the use of high-resolution urban morphology has been shown to increase modeled drag and heat flux (Shen et al., 2019), reducing their error against observed air temperature and wind (Sun et al., 2021). However, radiative parameters, which currently only U-Surf provides, also vary for urban surfaces and modulate urban microclimates (Best & Grimmond, 2015; Chakraborty et al., 2021). Since U-Surf was originally developed for a single-layer UCM embedded within the Community Land Model, its morphological parameters were developed for a structurally different UCM than the multilayer UCM within WRF. Here, we modify the U-Surf dataset to make it consistent with the urban structural assumptions in WRF and combine it with a gridded LCZ dataset to simulate recent extreme heat events in major U.S. cities.

In the following section, we provide an overview of the U-Surf dataset, our modifications to make it consistent with the WRF UCM, which we term U-Surf-WRF, and the experimental design to run our model simulations over multiple U.S. cities. We then validate our simulations with the updated U-Surf-WRF dataset to demonstrate its ability to capture the magnitude and spatial variability of urban heat, humidity, and heat stress signals. Finally, we discuss the potential for using spatially continuous urban parameters within WRF and future priorities to improve urban surface constraints in process-based models.

2 Methods

2.1 Cities and events of interest

Heatwave events for 13 major US cities were simulated (Fig 1a,d). For each city, we identified one heatwave between May 2015 and June 2024, spinning up the model for 72, 69, 66, 63, and 60 hours to generate five ensemble members. The heatwaves were selected by identifying the 3+ consecutive days where the mean air temperature was highest for each city during this period. Cases and cities are shown in Figure 1, along with key model configuration. More details are provided in section 2.3 below.

2.2 Brief description of the U-Surf dataset and development of U-Surf-WRF

The recently developed U-Surf dataset includes global 1 km facet-level estimates of several urban surface properties (Table 2.2) derived from several open-source datasets. Height-to-width ratio (H/W) is extracted from 3D-GloBFP (Che et al., 2024) and Microsoft building footprint data (Microsoft, 2022), plan area fraction (λ_p) is extracted from Microsoft building footprint data, and building height distribution is extracted from 3D-GloBFP. Radiative variables emissivity (ε) and albedo (α) are derived from ASTERv3 (Hulley et al., 2015) and Sentinel2 (Lin et al., 2022), respectively. Impervious fraction a)

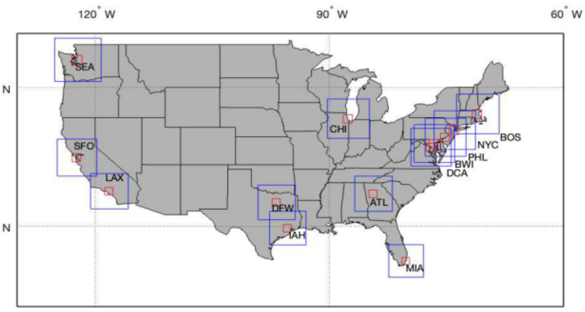

b)

Physics and dynamics options used in WRF

Urban physics	BEP-BEM (Salamanca et al., 2010)
Longwave	RRTM
Shortwave	Dudhia
Land	Noah
Microphysics	Thompson
Planetary boundary layer	BouLac
Resolution	$3km^2$, $1km^2$
Domain size	151x151, 100x100
AC adoption rate	50%
AC set point temperature	294.15 K

c)

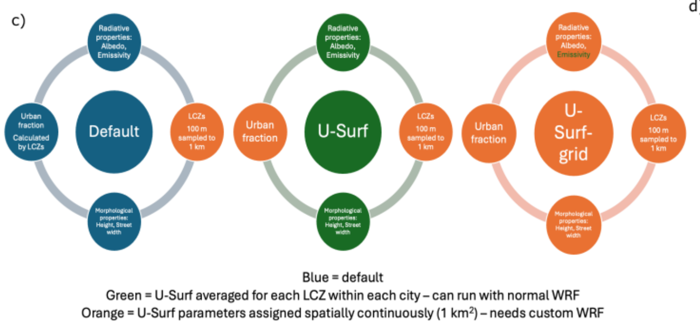

d)

Cities and corresponding heatwaves simulated

City	Abbreviation	Heatwave
Baltimore	bwi	19-21 Jul, 2019
Boston	bos	19-21 Jul, 2019
Philadelphia	phl	20-25 Jul, 2022
New York	nyc	21-23 Jul, 2021
Miami	mia	20-25 Jul, 2023
San Francisco	sfo	14-17 Oct, 2020
Seattle	sea	26-28 Jun, 2021
Dallas	dfw	18-21 Jul, 2018
Houston	iah	12-16 Aug, 2020
Los Angeles	lax	31 Aug - 8 Sep, 2022
Washington	dca	11-15 Aug, 2021
Chicago	chi	24-27 Aug, 2021
Atlanta	atl	21-27 Aug, 2023

Figure 1. Experimental design and model configuration. a) Inner (red) and outer (blue) WRF domains for each of the 13 cities simulated. b) Select WRF parameters and modules used in this study. c) Three experiments conducted in this study. Blue indicates default WRF values were used. Green indicates U-Surf values by LCZ were derived. Orange indicates spatially continuous U-Surf values were used. U-Surf-grid simulations were only conducted for Houston and Chicago. d) Cities, abbreviations, and heatwaves simulated in this study.

Table 1. Urban surface properties from U-Surf (Cheng et al., 2025) used in this study.

Roof albedo	α_r
Wall albedo	α_w
Ground albedo	α_g
Roof emissivity	ε_r
Wall emissivity	ε_w
Ground emissivity	ε_g
Urban fraction	λ_u
Height-to-width ratio	H/W
Plan area fraction	λ_p
Building height	H

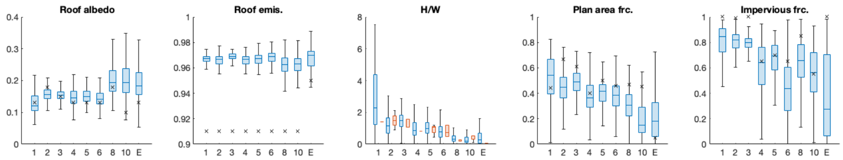

Figure 2. Select U-Surf urban properties (blue) compared with WRF defaults (orange bars and x's), aggregated by LCZ. Each data point is one grid square within administrative city limits for all of the 13 simulated cities. This figure is reproduced for each of the 13 individual simulated cities as figure A2

is extracted from ESA Worldcover v200 (Zanaga et al., 2022). For a complete description, the reader is referred to Cheng et al. (2025).

While ESMs such as the Community Earth System Model (CESM; (Danabasoglu et al., 2020)) and the U.S. Department of Energy's Energy Exascale Earth System Model (E3SM; (Golaz et al., 2022)) can ingest these urban parameters grid point by grid point, WRF urban parameters data are assigned by LCZ through a lookup table. As such, to run WRF with U-Surf, we aggregate the spatially continuous U-Surf data into LCZs that can then be used to update the lookup tables for each city (Demuzere et al., 2020).

Figure 2 compares U-Surf against WRF default data over the 13 simulated cities in aggregate (Section 2), and figure A2 shows the same information for each of the 13 individual cities. Broadly, U-Surf data exhibit greater variability than default data. Urban albedo is more variable between LCZs for U-Surf for most cities, although it is similarly variable when cities are analyzed in aggregate. Urban emissivity is consistently greater for U-Surf, which is realistic given that it is generally considered underestimated in the default set of WRF parameters (Chakraborty et al., 2021).

Morphological variables tend toward a lower urban density in U-Surf-WRF, especially for LCZ 6 (open lowrise). Therefore, we hypothesize that urban heat island intensities simulated using U-Surf parameters would be lower than those using default parameters, for that LCZ. However, this is not the case for LCZ 1, where most cities examined have a greater H/W and λ_p than WRF defaults. We note that U-Surf suggests a wider distribution of H/W than WRF defaults for almost all cities and LCZs.

We also note that for some variables, the range of values within an LCZ can be large, and that this variability is not captured within the LCZ framework as implemented in WRF, except for the height-to-width ratio and impervious fraction. Therefore, in section 3.6, we examine the error introduced by this limitation of the LCZ framework.

WRF simulates vegetated urban land such as lawns and parks separately from impervious urban surfaces. This differs from the UCM structure for which U-Surf was generated, where vegetated/pervious streets (e.g. lawns and bare soil) are considered part of the urban surface. Therefore, the H/W, λ_p, and λ_u were recalculated to make it consistent with WRF's UCM before they are ingested into WRF.

λ_u is modified by scaling it by 1 minus the fraction of pervious streets per urban area, which itself is equal to $\lambda_{rp}(1-\lambda_p)$, where λ_{rp} is the fraction of urban ground area that is pervious (taken from U-Surf). Therefore:

$$\lambda_{u,new} = \lambda_u(1 - \lambda_{rp} + \lambda_p \lambda_{rp}) \tag{1}$$

Similarly, λ_p is modified by considering that the amount of roof area stays the same, but the urban area that is being scaled as in Equation 1. That is, $\lambda_{p,new}\lambda_{u,new} = \lambda_p\lambda_u$ and so

$$\lambda_{p,new} = \frac{\lambda_p}{(1 - \lambda_{rp} + \lambda_p\lambda_{rp})} \tag{2}$$

The above is valid when the denominator of the plan area fraction is impervious area, as when λ_p is ingested by LCZ through URBPARM_LCZ.TBL. However, when λ_p is ingested into the URBPARAM variable (which allows for spatially continuous assignment of variables), WRF assumes that, consistent with NUDAPT standards, the denominator is not only impervious area but total area, urban and non-urban. Therefore, we have that:

$$\lambda_{p,urbparam} = \lambda_p\lambda_u \tag{3}$$

where λ_u is taken from U-Surf.

Finally, H/W is modified by applying equation 5 from Cheng et al. (2025), noting that the λ_w in their equation is inversely proportional to λ_u. Substituting the new values of λ_u and λ_p given by Equations 1 and 3 and simplifying yields:

$$H/W_{new} = \frac{H/W}{1 - \lambda_{rp}} \tag{4}$$

A comparison between the three different urban fraction fields (default, unmodified U-Surf, and modified U-Surf) and satellite imagery is presented in Figure 3 for select cities (figure A1 for the remaining cities), showing that the impervious fraction is more realistically captured using this approach than with the unmodified U-Surf or the default field. The modified U-Surf dataset appropriate for ingesting into WRF, which we name U-Surf-WRF, can be found at Jiang, Cheng, et al. (2025) .

2.3 Model configuration and boundary conditions

The WRF regional weather model version 4.3.3 was used to dynamically downscale ERA5 reanalysis data to 3 km (outer grid) and then 1 km (inner grid). The coupled BEP-BEM (Building Effect Parametrization and Building Energy Model) urban canopy and building energy model was used to simulate urban effects (Salamanca et al., 2010; Martilli et al., 2002). It is a multi-layer scheme and is considered the state-of-the-art urban canopy model in WRF. Simulation parameters are listed in Figure 1b.

For each simulation, two sets of urban parameter constraints were used: one with the default look-up table (”default” henceforth) and one with urban parameters given by the U-Surf data (”U-Surf” henceforth). The LCZ scheme (Stewart & Oke, 2012) was used to classify neighbourhoods at 100 m, and LCZ class data were extracted from Demuzere et al. (2020) . While the default cases’ impervious fraction fields were assigned from default values by LCZ using the w2w tool (Demuzere et al., 2021), those for the U-Surf cases were extracted from U-Surf following Section 2.2 and then resampled for each $1km^2$ grid in the inner domain. This incongruity between impervious fraction and other urban parameters fields is because it is common for WRF urban modeling practitioners to assign impervious fraction by grid point while using default properties via the URBPARM_LCZ.TBL input file. We comment further on this in section 3.6.3.

Select facet-level properties were given by U-Surf (Cheng et al., 2025), as shown in Figure 1b. Urban properties except H were derived by taking an urban-fraction-weighted

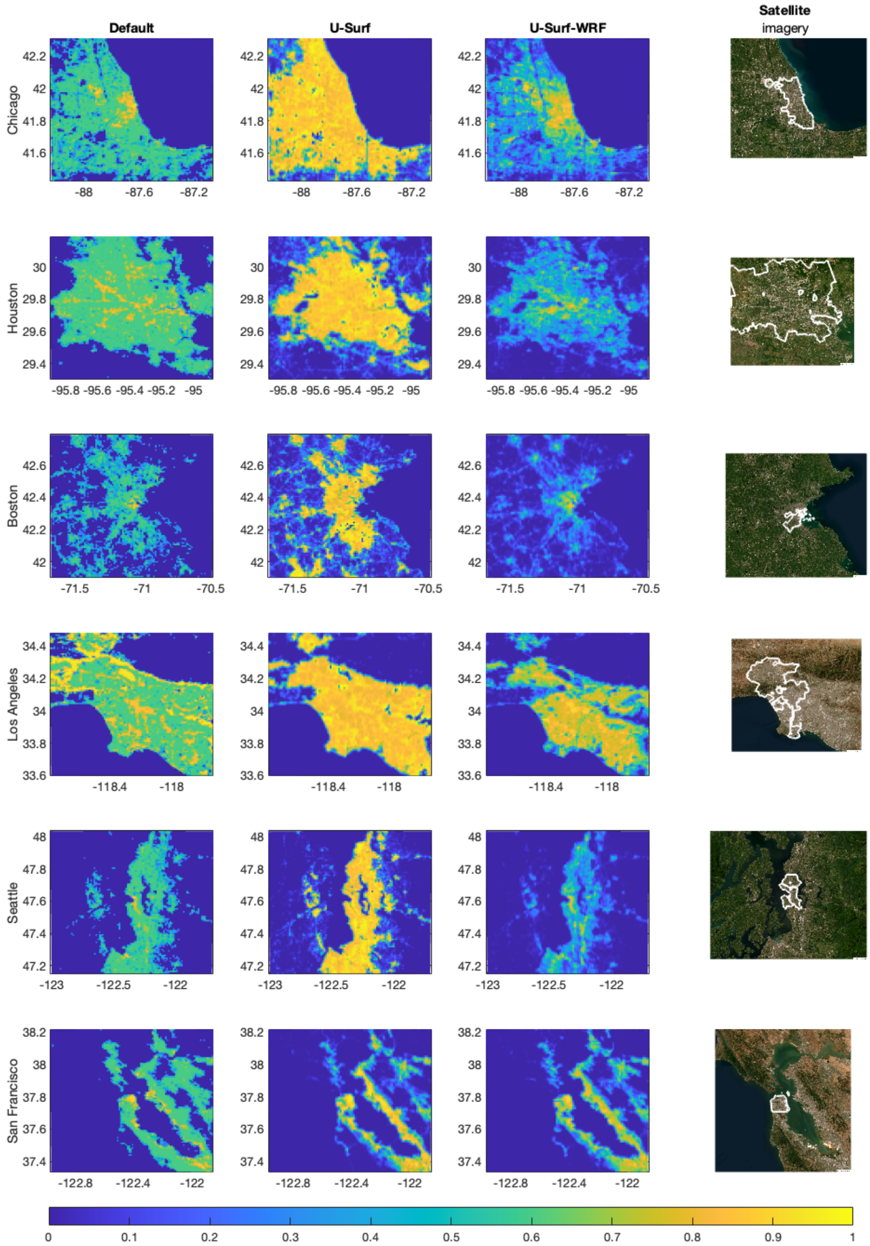

Figure 3. Urban fraction fields from default parameters, the unmodified U-Surf dataset, and the U-Surf dataset as modified in Section 2.2, compared with satellite imagery for select cities. This figure is produced for the remaining cities as figure A1.

average over each grid point within the city's administrative boundaries that corresponded to each LCZ. For example, for α_r for LCZ 2, we took the set of α_r values for all LCZ 2 grid points and weighted each point by λ_u. Building height distributions for each LCZ were derived from the λ_u-weighted distribution of the building heights for grid points in each LCZ, binned every 5 m (as is done in BEP-BEM).

In all sets of simulations, LULC data for non-urban areas were derived from Moderate Resolution Imaging Spectroradiometer (MODIS) data at a resolution of 15 arcseconds.

2.4 Simulations assigning spatially continuous urban parameters

By default, the WRF model is able to ingest certain urban parameters spatially continuously (i.e. grid point by grid point), including impervious fraction and building height distributions. In this study, for the purposes of validation (section 3.6.1) and sensitivity analysis (section 3.6.3), we use a modified WRF that ingests urban albedo (α_g, α_w, α_r) for each grid point as well *author:*~~(ref. for Alberto's code)~~(ref. for Alberto's code). Simulations for Chicago and Houston were conducted with all urban properties in Table 2.2 assigned for each grid point in the inner domain, except for ε, which is assigned city-specific U-Surf values by LCZ as the ASTER emissivity product used in U-Surf does not resolve large spatial variability within cities (figure 1c, A2). These simulations are referred to as "U-Surf-grid" henceforth.

Finally, for a more comprehensive sensitivity analysis, simulations for Chicago were conducted with only radiative (α_r,α_w,α_g), morphological (H/W,H,λ_p), or impervious fraction (λ_u) variables derived from U-Surf-WRF by LCZ (with all other variables with default settings) or for each grid point (with all other variables implemented by LCZ). Further details are presented in Section 3.6.3.

3 Results

3.1 Surface temperature validation for heat wave events

We first examine if using U-Surf-WRF improves model simulated urban land surface temperature (LST) against best available benchmarks. We choose to use satellite-derived LST from NASA's MODIS Aqua satellite as the benchmark since it provides daily estimates at our model's native resolution (1 km). We compare modeled against observed MODIS LST for each heatwave period for each city. Figure 4 shows that the intra-urban variability in each city is underestimated using default parameters, and that in most cases using the U-Surf parameters better captures the variability (r and slope closer to 1; Figure 4a,d) and lowers error (Figure 4b,f). Both default and U-Surf simulations tend to overestimate surface temperatures, but U-Surf tends to do so to a lesser extent (Figure 4c,g).

We note that surface temperature observations have limitations including limited valid data points during short time periods such as during the heatwaves, cloud cover and cloud shadows obscuring surfaces, thermal anisotropy, and algorithmic uncertainties. Model limitations include limited modes of variability (LCZs vs. spatially continuous grids) and lack of urban vegetation representation. To minimize some of these biases, we assess the performance of simulations for the summer climatology for Houston using various model configurations in section 3.6.1. Moreover, we further discuss several of these limitations in section . Nonetheless, it is encouraging that using U-Surf-WRF tends to bring simulations closer in line to satellite-derived LST observations.

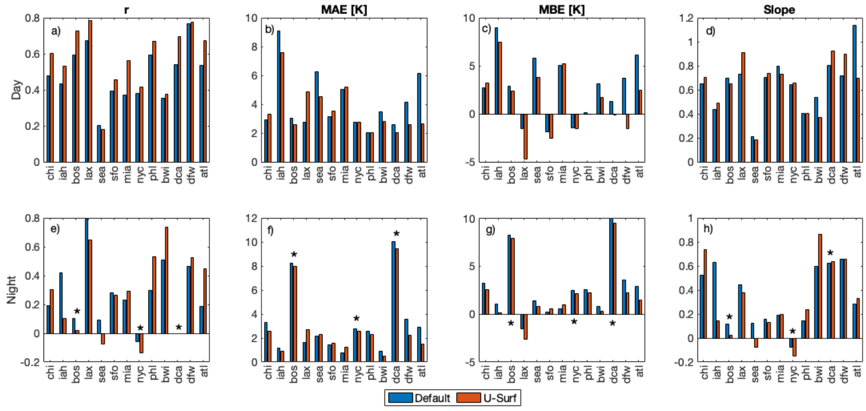

Figure 4. Model land surface temperature performance for each city's heatwave event. Summary statistics are shown for MODIS observed versus WRF simulated land surface temperature, where each data point is one $1km^2$ grid point. Day (a-d) refers to 13:30 local time, and Night (e-h) refers to 1:30 local time. An asterisk indicates that there were data available in the MODIS observations for fewer than 33% of grid points. Only two data points were available for dca at night, precluding a calculation of r.

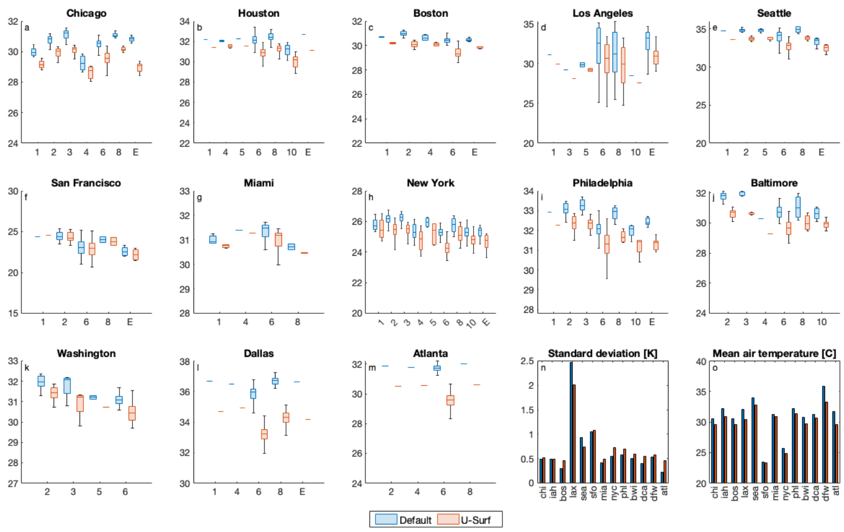

Figure 5. (a-m) Distribution of T_2 [∘C]by LCZ for each city, for both "default" and "U-Surf" simulations. Each point is one grid square ($1km^2$) within administrative city limits. (n) Standard deviation of T_2 for each city within administrative city limits. (o) Mean T_2 for each city within administrative city limits. Each point is one output time (30 minutes).

3.2 Simulating urban air temperature using U-Surf-WRF

Figure 5 shows the mean 2 m air temperature, T2, by LCZ for each of the 13 simulated cities, along with the standard deviation within the city boundaries. On average, T_2 is lower when simulated with U-Surf-WRF, and this result is robust for all simulated cities (Figure 5o). While each LCZ occupies a different place in each city (for example, closer to or farther away from the shore), precluding inter-LCZ comparison, the difference between default and U-Surf for each LCZ is often greatest for suburban LCZ 6. This is consistent with LCZ 6 having the greatest difference between U-Surf and default parameters (Figure A2).

In 11 of our 13 simulated cities, the spatial variability of T2 is greater for simulations using U-Surf-WRF during heatwaves (Figure 5n). Possible explanations include a larger range of impervious fractions throughout the city, a broader distribution of H/W within each LCZ, and a greater range of albedos between LCZs. However, the standard deviation of T2 is lower in Los Angeles under U-Surf. This is possibly because within the city boundary lie some forested and mountainous areas (Figure 3) which are cooler, so a lower urban air temperature would reduce the difference in air temperatures within the city boundaries.

Following mean T2, the daily maximum T2 exhibits similar variability for U-Surf-WRF simulations (Figure 6a). Conversely, at night, when the urban heat island effect is strongest, the minimum T2 varies more for default simulations (Figure 6b). This is consistent with default parameters representing heavier urban development, with corresponding stronger variability across LCZs.

3.3 Moisture and moist heat estimates

Simulated moisture (vapor pressure, e) for each city is greater using U-Surf-WRF compared to the default simulations (Figure 7). This is in part due to the greater built-up land in the default parameters compared to U-Surf-WRF, which replaces transpiring, vegetated land cover. Given that U-Surf-WRF tends to bring impervious fraction closer to the values seen in more heavily vegetated areas within city boundaries, such as parks and other recreational areas, we might expect the variation in moist heat to be lower compared to default. However, the variability is similar between the two sets of simulations.

The humidex (Government of Canada, 2002), a measure of humid heat and a function of both T2 and relative humidity, varies more than T2. We observe that, in certain cities, the expanded urban area used by default simulations (Figure 3) results in a much drier climate within city limits, as many points are represented as more heavily urbanized than reality in the model (Figure 8). This difference is seen mainly in the suburban areas of cities (Figure 8), where open lowrise (LCZ 6) areas are common, an LCZ whose urban intensity is particularly overestimated by WRF default parameters compared to U-Surf (Figure A2). The lower humidity in cities is a measure of the urban dry island effect, and is consistent with observational estimates (Chakraborty, Venter, et al., 2022), suggesting that, when we are concerned with moist heat, the lower simulated air temperature in suburbs when using U-Surf parameters may be partly compensated for by higher simulated humidity.

3.4 Urban-rural differences in temperature and heat stress

We compare urban (points within city limits with U-Surf impervious fraction $> 30\%$) and rural (land points in the $(100km)^2$ inner domain with U-Surf impervious fraction $< 5\%$) T2 to extract a local urban warming signal. We note that the rural reference sites for some cities are much higher in elevation than the corresponding urban area, so we caution that this may not be a true "urban heat island". However, here we primarily wish

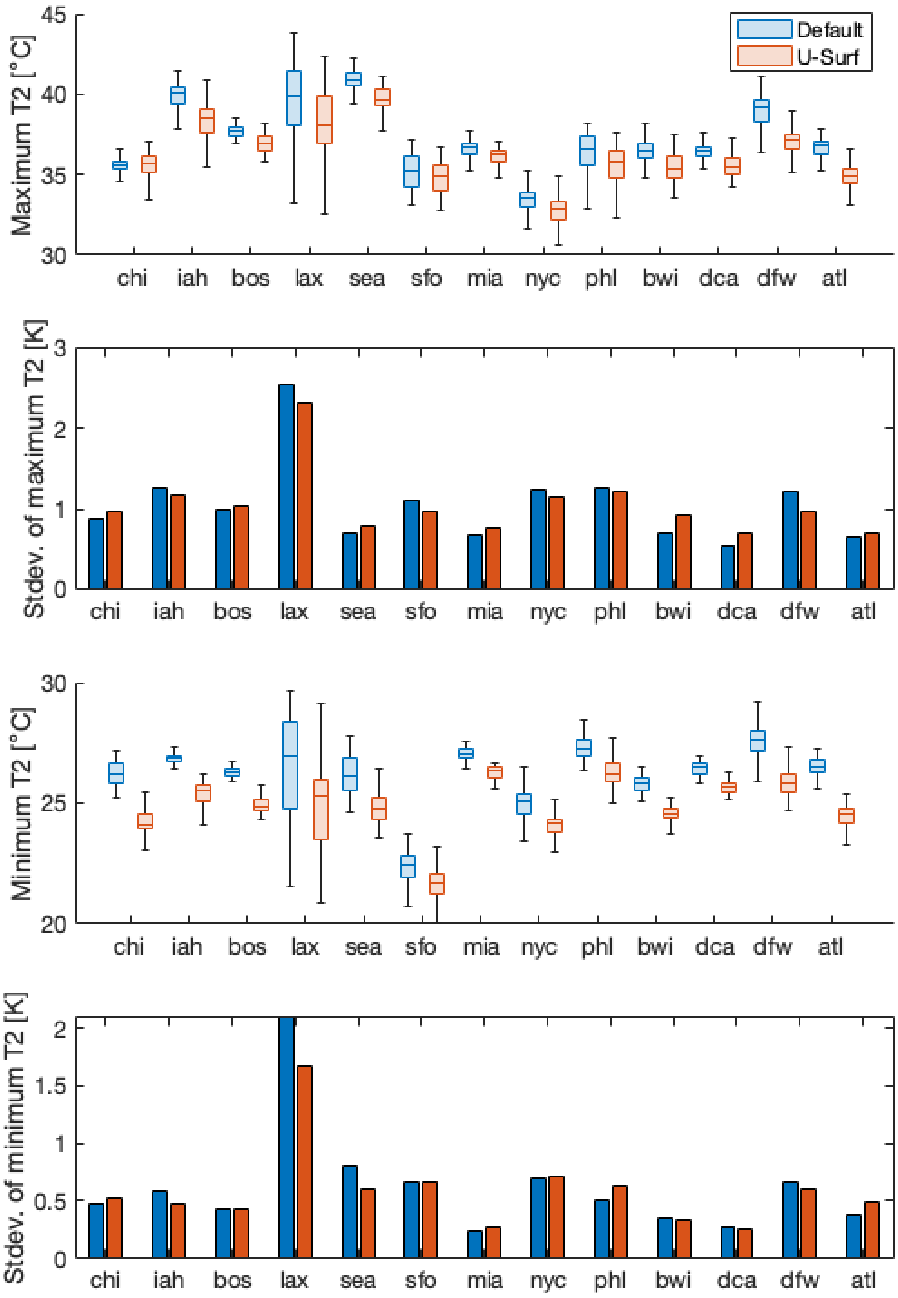

Figure 6. (a) Maximum and (c) minimum air temperature [$\circ$ C] simulated using default and U-Surf urban parameters, as well as their (b,d) spatial standard deviations, averaged over all days of each city's respective extreme heat event. Each point is one $1km^2$ grid square within administrative city limits.

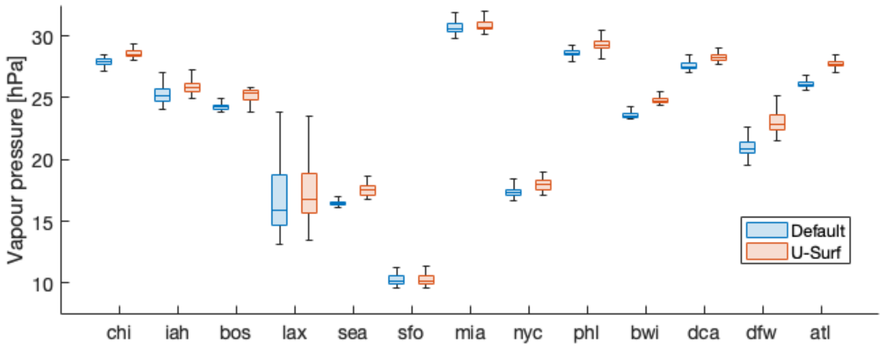

Figure 7. Vapour pressure [hPa] simulated using default and U-Surf urban parameters, averaged over all days of each city's respective extreme heat event. Each point is one $1km^2$ grid square within administrative city limits.

to examine effects thereon driven by using different urban parameters, not the magnitude of the heat island. During the heat waves, we find that using default parameters often yields greater estimates of the urban heat island. Estimates are especially higher at night, when the urban heat island is typically stronger. This result is robust for every city analyzed.

Cities tend to be drier during the day but not at night, consistent with Meili et al. (2022) . Compared to default, U-Surf simulates a moister urban-rural difference, robust in all cities at night and in 11 out of 13 cities during the day. As with many outcomes examined in this section, this can be attributed in part to the lower impervious fraction in U-Surf-WRF.

When considering moist heat stress, the competing effects of a moister but cooler city when using U-Surf-WRF may offset urban-rural differences, as Section 3.3 suggests. Indeed, in every city simulated, the difference between default and U-Surf-WRF simulations in an "urban humidex island" is less than that for air temperature urban heat island, although default WRF simulations still estimate higher values than U-Surf-WRF simulations.

3.5 Model sensitivity to individual urban parameters

In this section, we turn our attention to the individual U-Surf-WRF parameters' effects on T2 and humidity. We examine five different parameters (roof emissivity and albedo, impervious fraction, height-to-width ratio, and plan area fraction) and analyze the difference in T2 and e for corresponding differences in each of the parameters, over all cities' heatwave events.

Figure 10 shows that the greatest determinants of both air temperature and humidity differences between U-Surf and default simulations are H/W and impervious fraction, with R^2 at 10.5% and 10.4%, respectively, for T2 (10.2% and 10.5% for vapour pressure). We note that differences in H/W and impervious fraction are correlated in U-Surf, so the determination of the variance is lower than the sum of R^2 may suggest. Other variables appear to have weaker explanatory power, with R^2 between 1% and 4%. We suggest interpreting the low R^2 values not as an indication that other urban U-Surf parameter values are determining T_2 and e changes to a greater extent, but as other physical processes (e.g. advection – note the intercepts in Figure 10) or noise outweighing the local U-Surf signal from changes in these parameters.

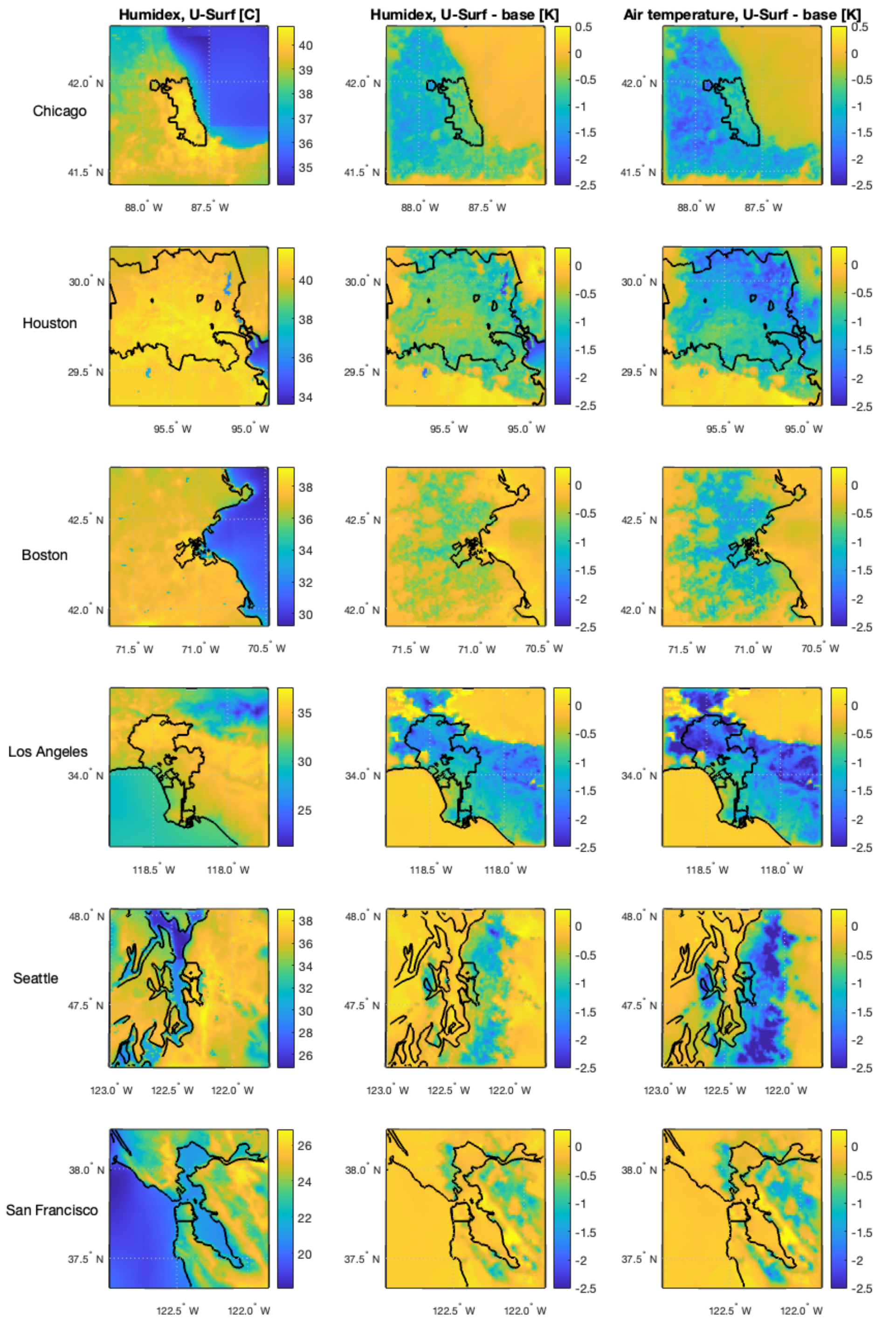

Figure 8. Humidex simulated using U-Surf urban parameters (left); difference in humidex between U-Surf and default simulations (centre); difference in air temperature between U-Surf and default simulations (right). This plot for the other 7 cities is produced in the Appendix as Figure A3

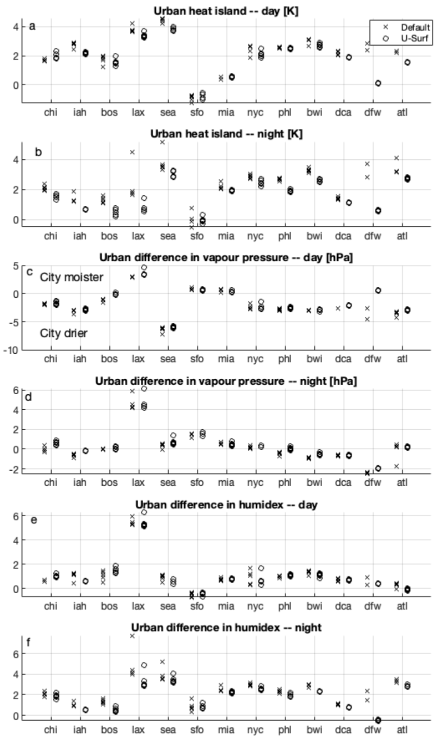

Figure 9. Urban-rural differences in 2 m air temperature, 2 m vapour pressure, and 2 m humidex, during the day (1:30 PM local time) and at night (1:30 AM local time). Each point is one ensemble member. "Urban" and "rural" are defined in the main text.

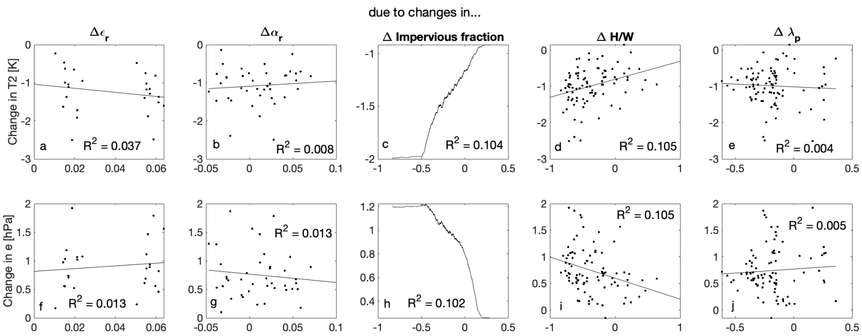

Figure 10. Differences in 2 m air temperature and 2 m vapour pressure between U-Surf and default simulations. Each LCZ for each city is one data point, except for (c,h), where each $1km^2$ grid square within city limits is one data point. (c,h) are processed using a 1000-point moving mean, while all other sub-figures display only the mean y-values for each unique x-value.

3.6 Implementing spatially continuous urban parameters into WRF-BEP-BEM

Earlier in section 3, all U-Surf-WRF data were assigned for each city by LCZ. However, U-Surf-WRF data are available at $1km^2$ resolution, so we examine here how implementing them not by LCZ but for each grid point affects urban heatwave simulations. The analyses in this section use U-Surf-WRF urban parameters that are assigned for every $1km^2$ grid point, ingested by a version of WRF modified to accept them. We call such simulations "U-Surf-grid".

3.6.1 Validation

In section 3.1, we evaluated model LST performance over heatwave periods against satellite observations. However, lack of data over many urban pixels, exacerbated by the short heatwave periods, may have led to a less robust evaluation. To that end, we perform a similar validation over a longer period and including U-Surf-grid. The summer of 2020 is simulated under default, U-Surf, and U-Surf-Grid for Houston. Daily surface temperatures at 1:30 AM and 1:30 PM within city limits, as well as their spatial variability, are assessed against MODIS satellite observations. Figure 11 shows that surface temperatures are more accurately captured under U-Surf-Grid during the day and U-Surf at night. Default parameters perform worst during both day and night.

We note that the slope in Figure 11a is shallower than in Figure 11b, indicating that default parameters more severely underestimate spatial variability in surface temperature than does U-Surf. At night, when urban effects are greatest, the U-Surf-Grid simulations yielded the greatest slope and R^2, indicating that U-Surf-Grid captures spatial variability in surface temperature better despite a higher mean absolute error (Figure 11f). Also, we note the clustering of simulated nighttime LST near 25 $\circ$C and 26 $\circ$C with U-Surf simulations for a wide range of observed LSTs, suggesting clustering by LCZs which we do not observe in U-Surf-Grid.

3.6.2 U-Surf-Grid versus U-Surf simulations for air temperature

In the previous section, we showed that spatial variability of LST is better captured when using spatially continuous parameters (U-Surf-Grid) at night compared to using city-specific parameters by LCZ except for impervious fraction (U-Surf). In this section, we examine how the simulations differ in terms of T2. We find that incorporating grid-wise urban parameters tends to very slightly increase simulated mean T2, similar to J. Chen et al. (2024) (Figure 12a), and we find slightly greater spatial variability when using U-Surf-Grid compared to U-Surf (Figure 12d). We find that the distribution of the changes in the maximum T2 skew negative while the changes in the minimum T2 skew positive. We also note that the distribution of changes in mean T2 is relatively narrow and small in the mean compared to the maximum and minimum T2, implying that the points with the greatest deviation in maximum air temperature tend to have the least deviation in minimum air temperature, and vice versa. This would be consistent with increased urban intensity and morphology explaining most of the signal. However, impervious fraction is already continuously assigned for "U-Surf" simulations. Therefore, we suggest that differences in urban morphology (i.e. height-to-width ratio and plan area fraction) are responsible for this spread.

3.6.3 Sensitivity analysis

To more comprehensively investigate the effects of assigning U-Surf properties in a spatially continuous manner, Chicago's heatwave event was simulated with different combinations of default, city-specific, and spatially continuous urban properties assignments for each variable. In addition to the three cases investigated in the rest of the manuscript

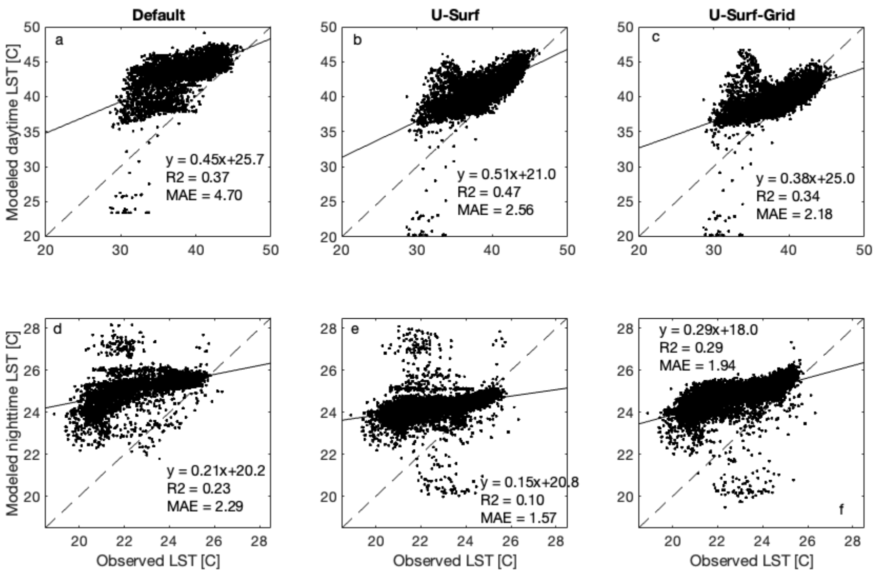

Figure 11. Modeled vs. observed LST for Houston summer 2020 at (a-c) 13:30 and (d-f) 1:30 local time. (a,d) are simulations using default parameters; (b,e) are U-Surf simulations using city-specific parameters by LCZ; and (c,f) are U-Surf-Grid simulations with parameters assigned spatially continuously for every grid point. Each data point corresponds to one $1km^2$ grid square.

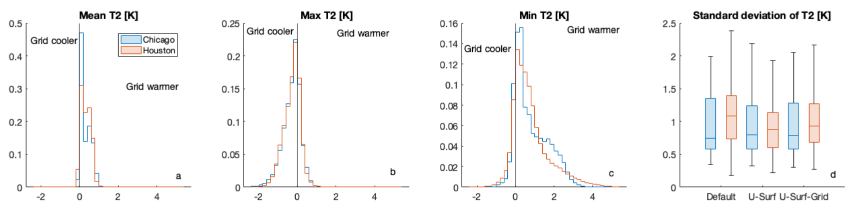

Figure 12. a-c) Distribution of simulated air temperature changes due to using U-Surf-Grid vs. U-Surf. "Max" and "min" T2 are taken at 1:30 PM and 1:30 AM local time, respectively. Each $1km^2$ grid square is one data point. d) Spatial standard deviation of T2 for default, U-Surf, and U-Surf-Grid simulations. Each 30-min time period for each of the 5 ensemble members is one data point.

(Default, U-Surf, and U-Surf-Grid), we introduce additional cases to diagnose which variables affect simulations the most, incrementally implementing U-Surf parameters by LCZ or in a spatially continuous manner. A common configuration in WRF model simulations is to assign impervious fraction for each grid point but to otherwise use default urban parameters, since WRF comes by default with NLCD impervious fraction data and a relatively easy way to ingest them. Therefore, we include also this configuration (10, BBG; see Figure 13) in our analysis.

Figure 13 illustrates the relative improvement for implementing each U-Surf product, by LCZ and spatially continuously. Here, B indicates default WRF values were used in the simulations, C indicates city-specific values derived from U-Surf were used for each LCZ, and G indicates spatially continuous values. The first letter of each case's name indicates radiative parameters α and ϵ, the second letter indicates morphological parameters H, H/W and λ_p, and the third letter indicates impervious fraction. Of special note are cases beginning with G (spatially continuous radiative parameters, cases 3 and 6): only α are spatially continuous, whereas ε are prescribed city-specific values by LCZ from U-Surf.

Broadly speaking, implementing spatially continuous U-Surf values (green bars) appears to reduce errors in surface temperatures to a greater extent than implementing them by LCZ (blue bars). LCZ-wise implementation of U-Surf makes LST simulations more accurate at night, but often makes them worse during the day. We find that assigning impervious fraction by grid point often makes only a marginal difference in the mean values, but that it often has a substantial effect in reducing the error in the spatial variability of the surface temperature. In contrast, LCZ-wise implementation of U-Surf properties does not improve simulated variability in surface temperature.

Spatially continuous implementation of U-Surf properties appears, by contrast, to offer additional improvements in simulating both air and surface temperature during the day compared to benchmarks. However, at night, there appears to be no substantial improvement over LCZ-wise assignment of U-Surf properties. This is surprising since urban effects are greater at night than during the day, and presumably also the effect of spatially continuous urban parameters. It suggests that cities – or at least Chicago during this extreme heat event – are more homogeneous at night than during the day, at least within LCZs.

Since albedo acts during the day and has only a residual effect at night, we expect improvements from implementing U-Surf albedo to be greater during the day than at night. We find that this is true for both air temperature and surface temperature (Figure 13e,f,i,j). However, this is not the case for the spatial variability, where benefits of spatially continuous U-Surf albedo are weak during the day, even to the point of reducing simulation accuracy. Recall that Chicago U-Surf albedo values vary to a greater extent than default values (Figure A2a). This may suggest that the spatial variability of albedo is overestimated. In contrast, spatial variability is better captured at night when using spatially continuously assigned albedo. This could arise if the variability is overestimated during the day but only a small part of it carries over to the night, helping simulation accuracy in terms of σ_T.

Next, we examine T2, noting that T2 comparisons are to the U-Surf-Grid simulations, which therefore introduces some error in this analysis, especially at night. We find that implementing U-Surf properties by LCZ improves agreement with the benchmark compared to default for mean temperatures and especially at night, but that it worsens accuracy during the day. However, implementation of any spatially continuous parameters (green bars) outperforms corresponding LCZ-based implementations for any time of day.

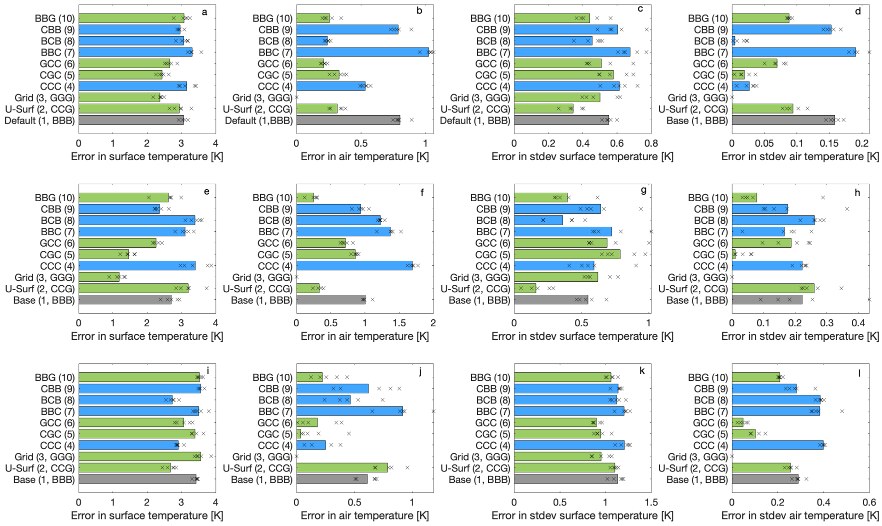

Figure 13. Added value from U-Surf products: mean (a-d; average of daytime and nighttime values), daytime (e-h; 1:30 PM local time), and nighttime (i-l; 1:30 AM local time) absolute deviations from reference values for Chicago's extreme heat period, provided from MODIS-AQUA observations for surface temperatures and from U-Surf-Grid simulations (3,GGG) for air temperatures. See main text for description of each bar. x's indicate individual ensemble members. Green bars indicate simulations with at least one component represented spatially continuously, while blue bars indicate simulations with at least one component using city-specific values by LCZ.

We also find that the common WRF urban modeling practice of assigning impervious cover in a spatially continuous manner but other urban properties set to their defaults performs (case 10) compares well to simulations with simulations using U-Surf urban properties assigned by LCZ (case 2) during the day and in the mean for surface temperature. For air temperature, keeping in mind the caveats above, it yields even closer results than case 2.

In summary, this analysis shows that, at least for Chicago during this extreme heat event, implementing spatially continuous urban parameters improves simulated air and surface temperatures, in general, with morphological parameters (H/W, λ_p) being more important for surface temperatures and facet-level albedo being more important for air temperatures. We also found that the common WRF practice of assigning spatially continuous impervious fraction and otherwise using default parameters may be adequate for simulations that are mostly interested in daytime results. Further analysis over a broader range of cities during a longer time period will advance our understanding of which urban parameters simulation outputs are most sensitive to in specific scenarios (e.g. cold or warm season), helping inform efforts to constrain urban parameters in a way that is fit for purpose.

4 Discussion

By using an ensemble of urban-resolving high-resolution WRF-BEP-BEM simulations for 13 major U.S. cities with different sets of urban parameters, we show the importance of representing city-specific urban surface constraints derived from spatially continuous observations in mesoscale weather simulations. In particular, we find that, using spatially continuous facet-level properties from the U-Surf dataset, the spatial variability generally increases (in 9 out of 13 cities), mean air temperature and humidex decrease (for all cities), and vapour pressure increases (for all cities). Correspondingly, urban-rural differences in heat and moisture decrease for all cities. When evaluated against LST observations for extreme heat events, U-Surf increases r (day: 12 out of 13 cities; night: 6 out of 10 cities) and decreases error (day: 8 out of 13 cities; night: 6 out of 10 cities); and when compared against LST observations for Houston summer 2020, U-Surf decreases error both when implemented by LCZ and by grid point. Results suggest that using default LCZ properties for every city does not fully leverage the LCZ framework. While the default values may be suitable for some urban modeling purposes, ideally parameters by LCZ for each city would be used. For example, an LCZ 4 neighbourhood may have a dense coverage of midrise buildings punctuated by an occasional tall building in one city, and in another be scattered tall buildings with flat ground in between. These two distributions of building heights, which can be captured with U-Surf, may lead to large differences in urban weather and climate simulations.

In the past, urban modelers had only one urban class or typology to work with. Finer model resolution and data increased the number of urban classes to 3 or 4 (usually low, medium, and high-intensity), then the 11 LCZ classes. Now, the state of the field of urban modeling is progressing toward assigning properties for each simulation grid square (as "U-Surf" cases do for impervious fraction), instead of aggregating by urban class (as "U-Surf" cases do for all other variables). An increasing number of urban canopy models, including those in CESM and E3SM, can ingest different urban parameters for every simulated urban grid point. J. Chen et al. (2024) found that modeled air temperature was on average not substantially different between simulations using parameters by LCZ and parameters assigned for every grid point, but that modeled minimum air temperature was more accurate. Here, we comprehensively assess this approach compared to the LCZ-based approach, informing efforts to develop models that can ingest data on this level (Figure 12). We do so by modifying the WRF base code to represent grid-wise urban albedo. Although this is not a capability that WRF has out-of-the-box, we encourage that this be included as a default option in future releases of WRF. We provide our modifications to the WRF source code to facilitate this in Jiang, Cheng, et al. (2025).

We also perform sensitivity analyses to understand the role of changing different urban properties, including facet-level albedo, emissivity, and morphology parameters on simulated temperature and humidity. Overall, we find that impervious fraction as well as building height are most important for accurately capturing near-surface urban climate and its spatial variability on the scale of our simulations (1-100 km). The default WRF parameters tend to overestimate this impervious fraction, especially in suburban areas, and the raw U-Surf dataset also severely overestimates this urban fraction (Figure 3), because it was designed for the UCM integrated in CESM with a different canopy structure. We modify this dataset to make it compatible with the structural assumptions in WRF, which we refer to as U-Surf-WRF and release for future use (Jiang, Cheng, et al., 2025). WRF's overestimated default urban parameters would lead to overestimations of the urban heat island and the urban dry island. These overestimations partially cancel out when calculating moist heat stress indices, though not completely (Figure 11). The overestimation of urban warming and other local meteorology in WRF is important to consider since it is the most common mesoscale model used in urban climate studies (Krayenhoff et al., 2021). With much of the literature also using these models to evaluate urban mitigation and adaptation strategies (Tan et al., 2024; Jiang, Krayenhoff, et al., 2025), we should be cautious in interpreting what these simulations tell us about the magnitudes and spatial variability of some of these effects. Moreover, these WRF simulations have also been used in conjunction with health and general socioeconomic (e.g. population distribution) data (Chakraborty, Wang, et al., 2023; K. Chen et al., 2022);

and if simulations overestimate urban warming, that risks an overestimation of urban impacts on various outcomes, like disparities in heat hazard. It might be fruitful to re-assess some of these results with more realistic impervious fraction as well as spatially continuous urban radiative and morphological parameters in the future.

With reference to the improvements in simulated variables seen on incorporating U-Surf-WRF, an important thing to note is that urban canopy models often have missing and unresolved processes, in addition to parametric uncertainties (which we try to address here) and structural assumptions that are simplistic for representing 'real' urban form. Many of these models have already been tuned to work reasonably well even with these uncertainties and missing processes. While we try to reduce uncertainties in the urban surface parameters using U-Surf-WRF, the existing model calibration may have been overcompensating for errors in other components. As such, even if the model performance degrades on using U-Surf-WRF, which happens in a minority of cases, that does not necessarily mean that the parameters are wrong. Rather, first constraining what can be reasonably constrained using globally scalable datasets presents an opportunity to figure out how the other components of the modeling framework had been hiding errors in past or default simulations.

For example, a major uncertainty in WRF and other urban-resolving regional climate models is the representation of urban vegetation. Multi-model comparisons have shown that models without explicit urban vegetation tend to underestimate latent heat flux (Lipson et al., 2024) and its impacts on associated meteorological variables. The representation of urban vegetation in regional climate models can be imprecise. Modelers have implemented urban vegetation in various ways, including simulating vegetation and urban areas separately (as in Noah; (Ek et al., 2003)) and simulating proxies for urban vegetation in the urban canyon (as in CTSM; (Lawrence et al., 2019)). In WRF, for example, the non-urban portion of urban grids are classified by default as "cropland mosaic", a mix of forests, grassland, shrubs, and cropland, when in practice different urban greenery is managed in a variety of different manners, varying from irrigated lawns and golf courses, to unmanaged forests to croplands.

Additionally, there often lacks urban vegetation data beyond a general "pervious" fraction. U-Surf represents urban parks, lawns, yards, and other vegetated surfaces into one category, "pervious road", simulated in CTSM's urban model similarly to bare soil. Street trees, distinct from forests and parks, are particularly affected by this dearth of data, even though they modulate several aspects of urban climate (Coleman et al., 2021; Krayenhoff et al., 2020; Salmond et al., 2016; Gromke & Ruck, 2009). However, while U-Surf provides the fraction of urban ground that is vegetated, it makes no attempt to capture street trees apart from other urban vegetation, possibly explaining why, even with U-Surf implemented, spatial variability in LST is still underestimated (Figure 4d,h). Even where there are urban vegetation and street tree data, they are often provided in a binary way (e.g. (Zanaga et al., 2022)), which when detected using low-resolution sensors may overestimate street tree cover in densely vegetated areas or underestimate it in sparsely vegetated areas. This poor handling of urban vegetation can be a major issue when trying to capture intra-urban variability in heat and heat stress, impacting estimates of disparities in heat hazard using process-based models (Chakraborty, Newman, et al., 2023; Chakraborty, Wang, et al., 2023). In contrast, observational estimates have shown that urban vegetation strongly modulates these disparities (Chakraborty, Biswas, et al., 2022; McDonald et al., 2021; Benz & Burney, 2021). Furthermore, even when vegetation data does exist for specific cities, models often lack the capability to ingest them, or have difficultly implementing them in a spatially coherent way.

Current urban vegetation products for climate and weather modeling also do not distinguish between the different types of urban vegetation (grass, shrubs, trees, and agriculture), a substantial limitation given the unique role that street trees play in modulating urban climate. For instance, Schwaab et al. (2021) found that urban trees reduce

LST substantially more than grass does. We may expect this discrepancy between tree-induced and grass-induced cooling to also exist for air temperature, though to a lesser extent (M. Du et al., 2024). Since WRF simulates the pervious fraction of each urban grid as "cropland mosaic", it could underestimate the spatial variability of urban heat and moisture, especially as the outermost urban grids tend to have more vegetation, including street tree cover in many cities. In this context, the < 1 slopes of the modeled vs satellite-observed LST data for most cities in our analysis (figure 4) make sense, as well as the warm LST bias even when U-Surf-WRF parameters are used. While previous studies have sometimes replaced how vegetation is represented in the pervious fraction of urban grid points to a single alternative LU class (e.g. to deciduous woodland in Brousse et al. (2024)), a more realistic approach would involve providing different dominant vegetation types for each urban point's pervious fraction. Another approach often used to estimate the impact of urban vegetation on weather and climate signals, especially in models without explicit urban vegetation, is to calculate a "true" urban signal by using weighted means of non-vegetated urban and natural grids in post-processing (Zhao et al., 2017). However, this implicitly assumes that urban vegetation is identical in form and function to that in background rural areas, which is untrue for many cases (Paschalis et al., 2021). While street tree and urban vegetation databases exist for individual cities, they are not universally available, and access and format limitations restrict their applicability for global or even regional-scale studies. Given this state of the modeling landscape, we urge the development of high-resolution street-tree and vegetation subtype products, possibly by leveraging satellite data, that vegetated UCMs can employ. In the same vein, we also encourage the development of UCMs that can capture the complex dynamics of urban vegetation in all its forms.

5 Conclusions

As satellite capabilities increase, providing climate modelers with a wealth of urban data, it is important to assess the value of undertaking the effort to implement them and to make sure they improve simulation fidelity. It is not entirely clear under which circumstances finer-resolution prescription of surface properties would result in more accurate simulations. In this study, we showed that implementing the satellite-derived U-Surf urban canyon parameters yielded greater model fidelity for most metrics and times of day, while improving outcomes less in other circumstances. For example, implementing U-Surf by LCZ increased modelled LST correlation with observations in 12 out of 13 cities during the day, but only 6 out of 10 cities at night. However, implementing U-Surf by grid points yielded a large improvement in modeled LST at night. With U-Surf, urban spatial variability was enhanced in 11 out of 13 cities, but in general remained underestimated although less severely so. U-Surf proved especially important when investigating urban-rural differences, where the magnitude of the effect is small, consistently yielding smaller nocturnal heat islands and daytime dry islands.

As with models, data must be fit for purpose. We found that bulk estimates of average urban air temperature may be well simulated through the common WRF practice of using default urban parameters but assigning urban fraction grid by grid. However, we demonstrated that incorporating varied urban parameters may be valuable in applications where intra-urban variability is of interest, especially of surface temperatures. We also envision applications investigating intra-city inequitable exposure to heat, especially during extreme heat events, which have disproportionate and nonlinear impacts on health and comfort (Gasparrini et al., 2015).

While the algorithms employed to generate global-scale urban parameter datasets are not adapted to any particular city or neighbourhood, it offers a baseline level of variability beyond what using default parameters offers. That is, city-specific datasets and observations will continue to be useful, but for national, continental, and global-scale studies, global-scale datasets derived from satellite observations can offer a level of accuracy in urban representation in regional climate models that generic LCZ parameters cannot. Therefore, we encourage the urban climate community to incorporate these spatially continuous estimates of urban canopy parameters in their simulations so as to more accurately capture the magnitude of urban heat, dry, and heat stress islands as well as their within-city variability. We also hope that the WRF community will continue to improve the model's capability to fully utilize such datasets for high-fidelity urban climate modeling. To facilitate this, we provide a global 1 km U-Surf-WRF product that is structurally consistent with WRF's urban canopy structure and code modifications to run WRF with grid-wise facet-level urban albedo and morphology parameters (Jiang, Cheng, et al., 2025).

654 # Appendix A Figures for additional cities analyzed

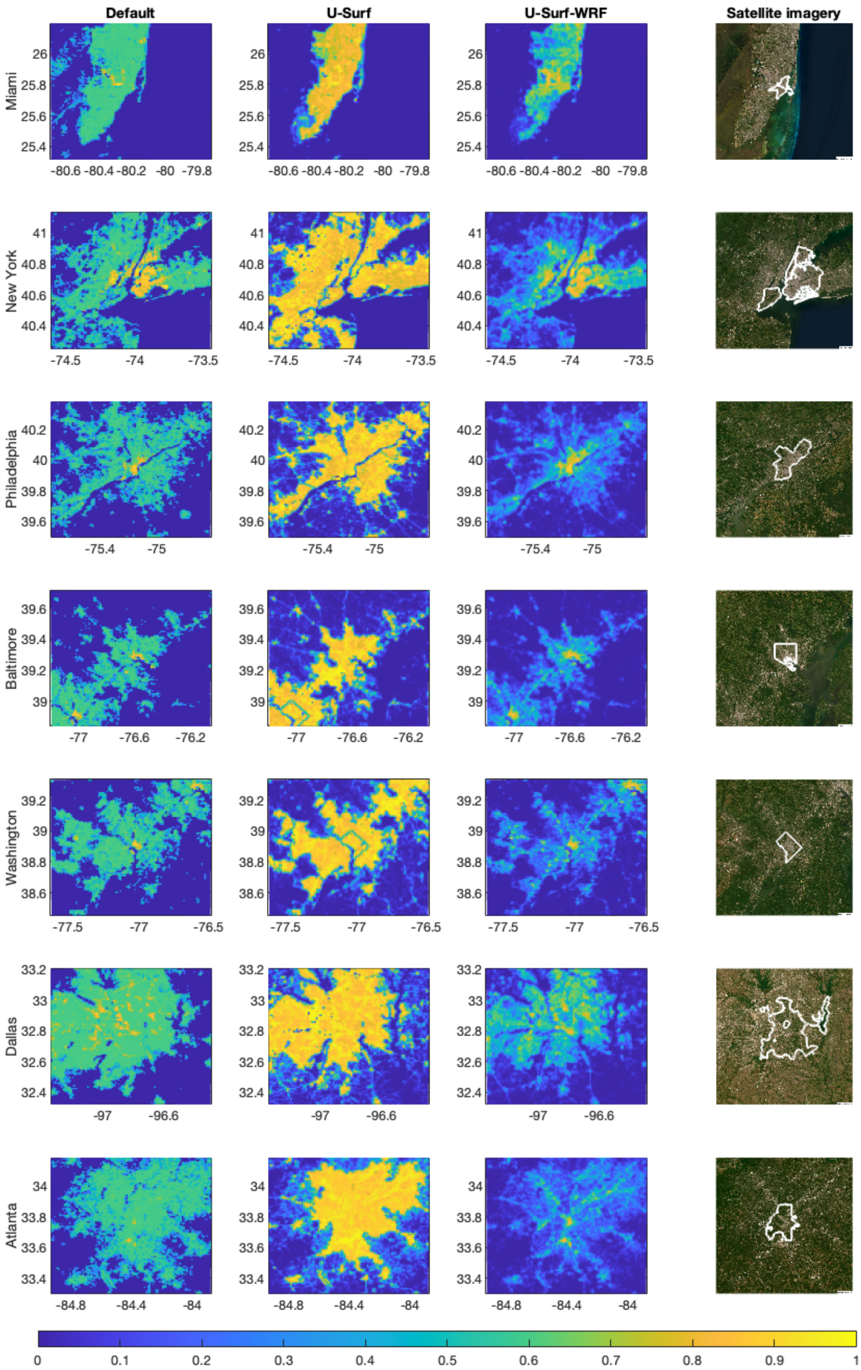

Figure A1. As Figure 3, but for the remaining 7 examined cities.

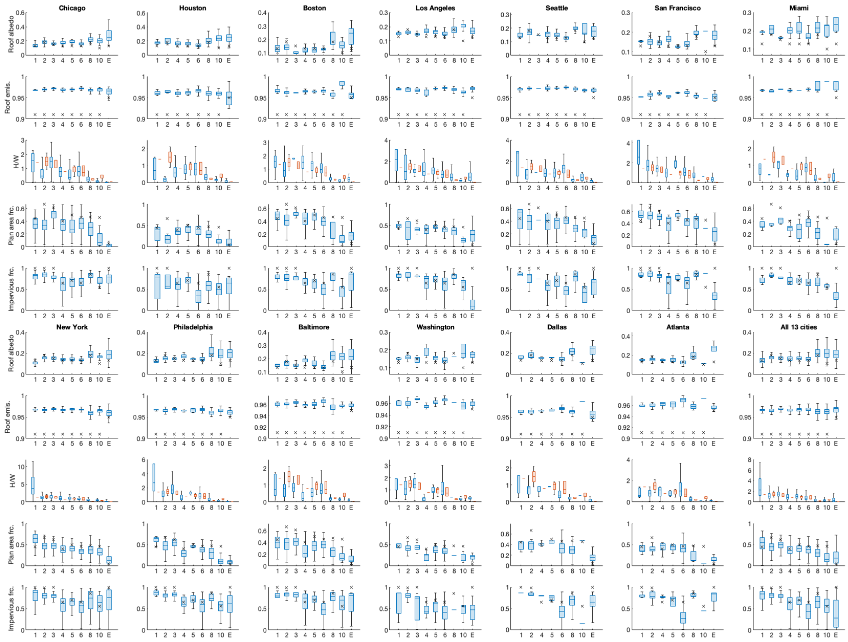

Figure A2. Select urban properties (blue) compared with WRF defaults (orange bars and x's). Each data point is one grid square within administrative city limits for each of the 13 simulated cities.

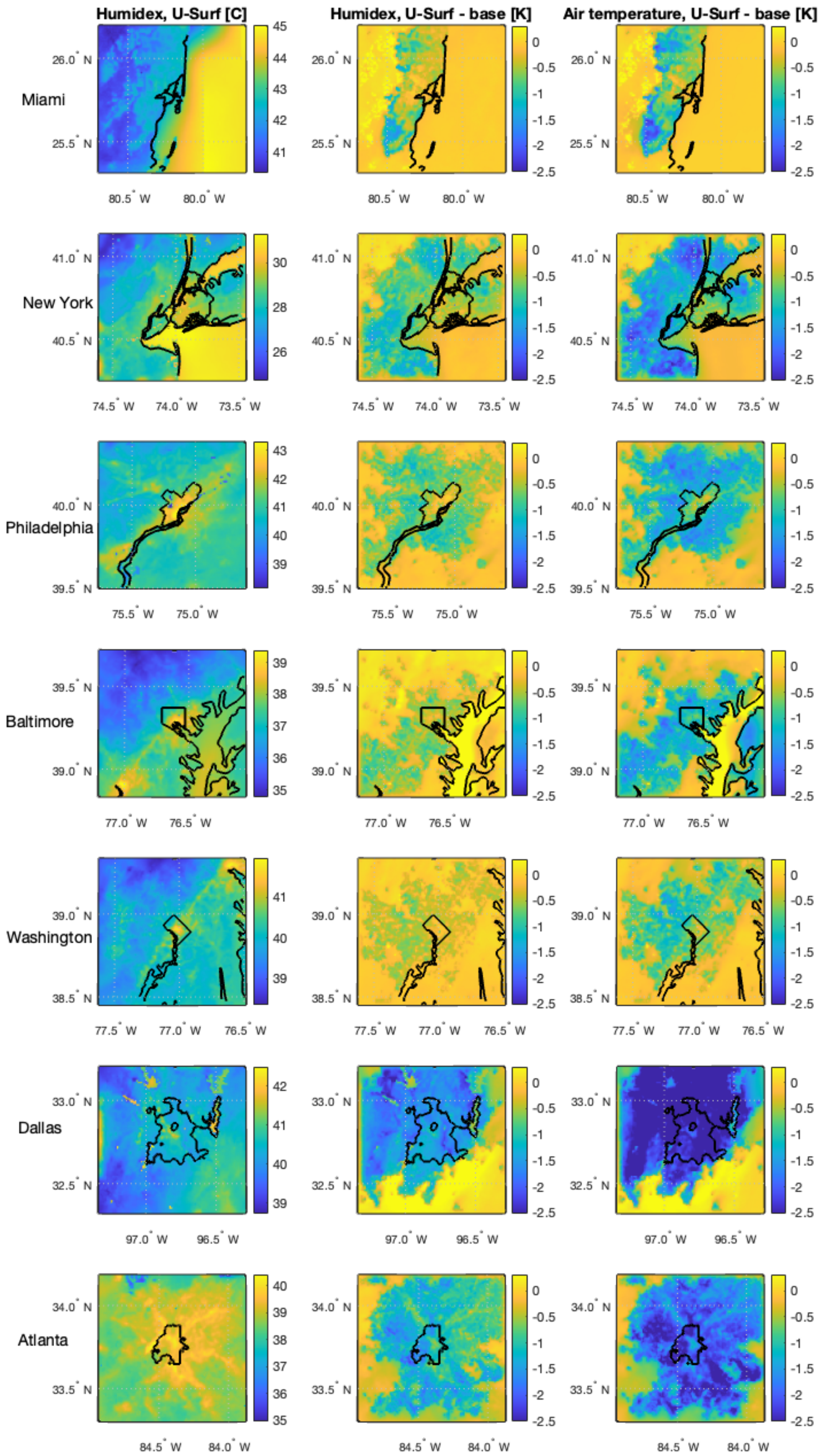

Figure A3. As Figure 8, for the remaining 7 cities.

Open Research Section

Code from WRF version 4.3.3, data from U-Surf can be accessed through links in the bibliography. U-Surf data that have been modified for use with WRF, as described in section 2.2, can be accessed at Jiang, Cheng, et al. (2025). Modifications to WRF to allow it to ingest grid-by-grid urban albedo can also be accessed at Jiang, Cheng, et al. (2025).

Author contributions

T.C. conceptualized the study, acquired funding, provided supervision, and estimated the land surface temperature from satellite data. T.J. designed and conducted the model simulations and analyzed all the data. Y.C., R.M., T.C., and L.Z. provided and processed input facet-level urban parameters underlying this study. A.M. modified the source code for the WRF model to allow use of grid-wise urban parameters. T.J. and T.C. wrote the initial draft of this manuscript. All authors reviewed and edited the manuscript.

Acknowledgments
This work was supported jointly by the Earth System Model Development and Regional and Global Model Analysis program areas of the Biological and Environmental Research program of the U.S. Department of Energy (DOE), Office of Science through an Early Career Research Program Award to T.C. A.M.'s contribution has been supported by the CROCUS project funded by DOE BER (grant no. DE-FOA-0002581). Pacific Northwest National Laboratory is operated for DOE by Battelle Memorial Institute under contract DE-AC05-76RL01830. This research used resources of the National Energy Research Scientific Computing Center, a DOE Office of Science User Facility supported by the Office of Science of the DOE under Contract No. DE-AC02-05CH11231 using NERSC award BER-ERCAP0031684. Computational resources for this research were also provided by COMPASS, a coastal research program funded by the Biological and Environmental Science Program of the DOE Office of Science.

References

Arnfield, A. J. (2003). Two decades of urban climate research: a review of turbulence, exchanges of energy and water, and the urban heat island. *International Journal of Climatology*, *23*(1), 1–26. doi: 10.1002/joc.859

Benz, S. A., & Burney, J. A. (2021). Widespread Race and Class Disparities in Surface Urban Heat Extremes Across the United States. *Earth's Future*, *9*(7), e2021EF002016. doi: 10.1029/2021EF002016

Best, M. J., & Grimmond, C. S. B. (2015). Key conclusions of the first international urban land surface model comparison project. *Bulletin of the American Meteorological Society*, *96*(5), 805–819.

Brousse, O., Simpson, C., Zonato, A., Martilli, A., Taylor, J., Davies, M., & Heaviside, C. (2024). Cool Roofs Could Be Most Effective at Reducing Outdoor Urban Temperatures in London (United Kingdom) Compared With Other Roof Top and Vegetation Interventions: A Mesoscale Urban Climate Modeling Study. *Geophysical Research Letters*, *51*(13), e2024GL109634. doi: 10.1029/2024GL109634

Chakraborty, T., Biswas, T., Campbell, L. S., Franklin, B., Parker, S. S., & Tukman, M. (2022). Feasibility of afforestation as an equitable nature-based solution in urban areas. *Sustainable Cities and Society*, *81*, 103826.

Chakraborty, T., Lee, X., Ermida, S., & Zhan, W. (2021). On the land emissivity assumption and Landsat-derived surface urban heat islands: A global analysis. *Remote Sensing of Environment*, *265*, 112682.

Chakraborty, T., Newman, A. J., Qian, Y., Hsu, A., & Sheriff, G. (2023). Residential segregation and outdoor urban moist heat stress disparities in the United States. *One Earth*, *6*(6), 738–750.

Chakraborty, T., & Qian, Y. (2024). Urbanization exacerbates continental-to regional-scale warming. *One Earth*, *7*(8), 1387–1401.

Chakraborty, T., Venter, Z. S., Qian, Y., & Lee, X. (2022). Lower Urban Humidity Moderates Outdoor Heat Stress. *AGU Advances*, *3*(5), e2022AV000729. doi: 10.1029/2022AV000729

Chakraborty, T., Wang, J., Qian, Y., Pringle, W., Yang, Z., & Xue, P. (2023). Urban Versus Lake Impacts on Heat Stress and Its Disparities in a Shoreline City. *GeoHealth*, *7*(11), e2023GH000869. doi: 10.1029/2023GH000869

Che, Y., Li, X., Liu, X., Wang, Y., Liao, W., Zheng, X., … Dai, Y. (2024). 3D-GloBFP: the first global three-dimensional building footprint dataset. *Earth System Science Data*, *16*(11), 5357–5374. doi: 10.5194/essd-16-5357-2024

Chen, J., Dong, N., Liu, Z., Chen, Y., Luo, M., & Huang, H. (2024). Local temperature impact of urban heat mitigation strategy based on WRF integrating urban canopy parameters and local climate zones. *Building and Environment*, 112257. doi: 10.1016/j.buildenv.2024.112257

Chen, K., Newman, A. J., Huang, M., Coon, C., Darrow, L. A., Strickland, M. J., & Holmes, H. A. (2022). Estimating Heat-Related Exposures and Urban Heat Island Impacts: A Case Study for the 2012 Chicago Heatwave. *GeoHealth*, *6*(1), e2021GH000535. doi: 10.1029/2021GH000535

Cheng, Y., Zhao, L., Chakraborty, T., Oleson, K., Demuzere, M., Liu, X., … Li, X. C. (2025). U-surf: a global 1 km spatially continuous urban surface property dataset for kilometer-scale urban-resolving earth system modeling. *Earth System Science Data*, *17*(5), 2147–2174.

Ching, J., Mills, G., Bechtel, B., See, L., Feddema, J., Wang, X., … Theeuwes, N. (2018). WUDAPT: An Urban Weather, Climate, and Environmental Modeling Infrastructure for the Anthropocene. *Bulletin of the American Meteorological Society*, *99*(9), 1907 – 1924. doi: 10.1175/BAMS-D-16-0236.1

Coleman, A. F., Ryan, R. L., Eisenman, T. S., Locke, D. H., & Harper, R. W. (2021). The influence of street trees on pedestrian perceptions of safety: Results from environmental justice areas of Massachusetts, U.S. *Urban Forestry & Urban Greening*, *64*, 127258. doi: 10.1016/j.ufug.2021.127258

Danabasoglu, G., Lamarque, J., Bacmeister, J., Bailey, D. A., DuVivier, A. K., Edwards, J., … Strand, W. G. (2020). The Community Earth System Model Version 2 (CESM2). *Journal of Advances in Modeling Earth Systems*, *12*(2), e2019MS001916. doi: 10.1029/2019MS001916

Demuzere, M., Argüeso, D., Zonato, A., & Kittner, J. (2022). W2W: A Python package that injects WUDAPT's LocalClimate Zone information in WRF. *Journal of Open Source Software*, *7*(76), 4432. doi: 10.21105/joss.04432

Demuzere, M., Hankey, S., Mills, G., Zhang, W., Lu, T., & Bechtel, B. (2020). Combining expert and crowd-sourced training data to map urban form and functions for the continental US. *Scientific Data*, *7*(1), 264. doi: 10.1038/s41597-020-00605-z

Demuzere, M., Kittner, J., & Bechtel, B. (2021). LCZ Generator: a web application to create Local Climate Zone maps. *Frontiers in Environmental Science*, *9*, 637455.

Du, H., Zhan, W., Zhou, B., Ju, Y., Liu, Z., Middel, A., … Wang, Z. (2025). Exacerbated heat stress induced by urban browning in the Global South. *Nature Cities*, 1–13.

Du, M., Li, N., Hu, T., Yang, Q., Chakraborty, T., Venter, Z., & Yao, R. (2024). Daytime cooling efficiencies of urban trees derived from land surface temperature are much higher than those for air temperature. *Environmental Research Letters*, *19*(4), 044037.

Ek, M. B., Mitchell, K. E., Lin, Y., Rogers, E., Grunmann, P., Koren, V., ... Tarpley, J. D. (2003). *Implementation of Noah land surface model advances in the National Centers for Environmental Prediction operational mesoscale Eta model* (Vol. 108) (No. D22). doi: 10.1029/2002JD003296

Gasparrini, A., Guo, Y., Hashizume, M., Lavigne, E., Zanobetti, A., Schwartz, J., ... Armstrong, B. (2015). Mortality risk attributable to high and low ambient temperature: a multicountry observational study. *The Lancet*, *386*(9991), 369–375. doi: 10.1016/S0140-6736(14)62114-0

Golaz, J., Van Roekel, L. P., Zheng, X., Roberts, A. F., Wolfe, J. D., Lin, W., ... Bader, D. C. (2022). The DOE E3SM Model Version 2: Overview of the Physical Model and Initial Model Evaluation. *Journal of Advances in Modeling Earth Systems*, *14*(12), e2022MS003156. doi: 10.1029/2022MS003156

Government of Canada, P. S. a. P. C. (2002). *Humidex : a method of quantifying human discomfort due to excessive heat and humidity / by J.M. Masterson and F.A. Richardson.: En57-23/1-79E-PDF - Government of Canada Publications - Canada.ca.*

Gromke, C., & Ruck, B. (2009). On the Impact of Trees on Dispersion Processes of Traffic Emissions in Street Canyons. *Boundary-Layer Meteorology*, *131*(1), 19–34. doi: 10.1007/s10546-008-9301-2

Hamdi, R., Degrauwe, D., & Termonia, P. (2012). Coupling the Town Energy Balance (TEB) Scheme to an Operational Limited-Area NWP Model: Evaluation for a Highly Urbanized Area in Belgium. *Weather and Forecasting*. doi: 10.1175/WAF-D-11-00064.1

Hulley, G. C., Hook, S. J., Abbott, E., Malakar, N., Islam, T., & Abrams, M. (2015). The ASTER Global Emissivity Dataset (ASTER GED): Mapping Earth's emissivity at 100 meter spatial scale. *Geophysical Research Letters*, *42*(19), 7966–7976. doi: 10.1002/2015GL065564

Jackson, T. L., Feddema, J. J., Oleson, K. W., Bonan, G. B., & Bauer, J. T. (2013). Parameterization of urban characteristics for global climate modeling. In *Geography of climate change* (pp. 135–152). Routledge.

Jiang, T., Cheng, Y., Mukherjee, R., Chakraborty, T., Zhao, L., & Martilli, A. (2025). *U-Surf-WRF: Modifications to U-Surf and the WRF Model for Compatibility.* Zenodo, doi: 10.5281/zenodo.15217359.

Jiang, T., Krayenhoff, E. S., Martilli, A., Nazarian, N., Stone, B., & Voogt, J. A. (2025). Prioritizing urban heat adaptation infrastructure based on multiple outcomes: Comfort, health, and energy. *Proceedings of the National Academy of Sciences*, *122*(19), e2411144122. doi: 10.1073/pnas.2411144122

Kamath, H. G., Singh, M., Malviya, N., Martilli, A., He, L., Aliaga, D., ... Niyogi, D. (2024). GLObal Building heights for Urban Studies (UT-GLOBUS) for city- and street- scale urban simulations: Development and first applications. *Scientific Data*, *11*(1), 886. doi: 10.1038/s41597-024-03719-w

Krayenhoff, E. S., Broadbent, A. M., Zhao, L., Georgescu, M., Middel, A., Voogt, J. A., ... Erell, E. (2021). Cooling hot cities: a systematic and critical review of the numerical modelling literature. *Environmental Research Letters*, *16*(5), 053007.

Krayenhoff, E. S., Jiang, T., Christen, A., Martilli, A., Oke, T. R., Bailey, B. N., ... Stastny, A. (2020). A multi-layer urban canopy meteorological model with trees (BEP-Tree): Street tree impacts on pedestrian-level climate. *Urban Climate*, *32*, 100590.

Lawrence, D. M., Fisher, R. A., Koven, C. D., Oleson, K. W., Swenson, S. C., Bonan, G., ... Zeng, X. (2019). The Community Land Model Version 5: Description of New Features, Benchmarking, and Impact of Forcing Uncertainty. *Journal of Advances in Modeling Earth Systems*, *11*(12), 4245–4287. doi: 10.1029/2018MS001583

Li, R., Sun, T., Ghaffarian, S., Tsamados, M., & Ni, G. (2024). GLAMOUR:

GLobAl building MOrphology dataset for URban hydroclimate modelling. *Scientific Data*, *11*(1), 618. doi: 10.1038/s41597-024-03446-2

Liao, W., Li, Y., Liu, X., Wang, Y., Che, Y., Shao, L., … Chen, F. (2024). GloUCP: A global 1 km spatially continuous urban canopy parameters for the WRF model. *Earth System Science Data Discussions*, 1–21. doi: 10.5194/essd-2024-408

Lin, X., Wu, S., Chen, B., Lin, Z., Yan, Z., Chen, X., … Liu, Q. (2022). Estimating 10-m land surface albedo from Sentinel-2 satellite observations using a direct estimation approach with Google Earth Engine. *ISPRS Journal of Photogrammetry and Remote Sensing*, *194*, 1–20.

Lipson, M. J., Grimmond, S., Best, M., Abramowitz, G., Coutts, A., Tapper, N., … Pitman, A. J. (2024). Evaluation of 30 urban land surface models in the Urban-PLUMBER project: Phase 1 results. *Quarterly Journal of the Royal Meteorological Society*, *150*(758), 126–169. doi: 10.1002/qj.4589

Liu, Z., Zhan, W., Bechtel, B., Voogt, J., Lai, J., Chakraborty, T., … Lee, X. (2022). Surface warming in global cities is substantially more rapid than in rural background areas. *Communications Earth & Environment*, *3*(1), 219.

Martilli, A., Clappier, A., & Rotach, M. W. (2002). An Urban Surface Exchange Parameterisation for Mesoscale Models. *Boundary-Layer Meteorology*, *104*(2), 261–304. doi: 10.1023/A:1016099921195

McDonald, R. I., Biswas, T., Sachar, C., Housman, I., Boucher, T. M., Balk, D., … Leyk, S. (2021). The tree cover and temperature disparity in US urbanized areas: Quantifying the association with income across 5,723 communities. *PloS one*, *16*(4), e0249715.

Meili, N., Paschalis, A., Manoli, G., & Fatichi, S. (2022). Diurnal and seasonal patterns of global urban dry islands. *Environmental Research Letters*, *17*(5), 054044. doi: 10.1088/1748-9326/ac68f8

Microsoft. (2022). *Microsoft Planetary Computer.* Retrieved from `https://github.com/microsoft/GlobalMLBuildingFootprints`

Newman, A. J., Kalb, C., Chakraborty, T., Fitch, A., Darrow, L. A., Warren, J. L., … Chang, H. H. (2024). The High-resolution Urban Meteorology for Impacts Dataset (HUMID) daily for the Conterminous United States. *Scientific Data*, *11*(1), 1–16.

Oleson, K. W., & Feddema, J. (2020). Parameterization and Surface Data Improvements and New Capabilities for the Community Land Model Urban (CLMU). *Journal of Advances in Modeling Earth Systems*, *12*(2), e2018MS001586. doi: 10.1029/2018MS001586

Paschalis, A., Chakraborty, T., Fatichi, S., Meili, N., & Manoli, G. (2021). Urban Forests as Main Regulator of the Evaporative Cooling Effect in Cities. *AGU Advances*, *2*(2), e2020AV000303. doi: 10.1029/2020AV000303

Qian, Y., Chakraborty, T., Li, J., Li, D., He, C., Sarangi, C., … Leung, L. R. (2022). Urbanization Impact on Regional Climate and Extreme Weather: Current Understanding, Uncertainties, and Future Research Directions. *Advances in Atmospheric Sciences*, *39*(6), 819–860. doi: 10.1007/s00376-021-1371-9

Salamanca, F., Krpo, A., Martilli, A., & Clappier, A. (2010). A new building energy model coupled with an urban canopy parameterization for urban climate simulations—part I. formulation, verification, and sensitivity analysis of the model. *Theoretical and Applied Climatology*, *99*(3-4), 331–344. doi: 10.1007/s00704-009-0142-9

Salmond, J. A., Tadaki, M., Vardoulakis, S., Arbuthnott, K., Coutts, A., Demuzere, M., … Wheeler, B. W. (2016). Health and climate related ecosystem services provided by street trees in the urban environment. *Environmental Health*, *15*(S1), S36. doi: 10.1186/s12940-016-0103-6

Schwaab, J., Meier, R., Mussetti, G., Seneviratne, S., Bürgi, C., & Davin, E. L. (2021). The role of urban trees in reducing land surface temperatures in European cities. *Nature communications*, *12*(1), 6763.

Sharma, A., Wuebbles, D. J., & Kotamarthi, R. (2021). The Need for Urban-Resolving Climate Modeling Across Scales. *AGU Advances*, *2*(1), e2020AV000271. doi: 10.1029/2020AV000271

Shen, C., Chen, X., Dai, W., Li, X., Wu, J., Fan, Q., . . . Li, W. (2019). Impacts of High-Resolution Urban Canopy Parameters within the WRF Model on Dynamical and Thermal Fields over Guangzhou, China. doi: 10.1175/JAMC-D-18-0114.1

Stewart, I. D., & Oke, T. R. (2012). Local climate zones for urban temperature studies. *Bulletin of the American Meteorological Society*, *93*(12), 1879–1900.

Stokes, E. C., & Seto, K. C. (2019). Characterizing and measuring urban landscapes for sustainability. *Environmental Research Letters*, *14*(4), 045002.

Sun, Y., Zhang, N., Miao, S., Kong, F., Zhang, Y., & Li, N. (2021). Urban Morphological Parameters of the Main Cities in China and Their Application in the WRF Model. *Journal of Advances in Modeling Earth Systems*, *13*(8), e2020MS002382. doi: 10.1029/2020MS002382

Tan, H., Kotamarthi, R., Martilli, A., Fytanidis, D., & Dai, X. (2024). *Impact of Urban Parameters on Microclimate Conditions and Building Energy Consumption over Chicago Metropolitan Area during an Extreme Heatwave Event.* doi: 10.20944/preprints202407.2459.v1

Tuholske, C., Caylor, K., Funk, C., Verdin, A., Sweeney, S., Grace, K., . . . Evans, T. (2021). Global urban population exposure to extreme heat. *Proceedings of the National Academy of Sciences*, *118*(41), e2024792118. doi: 10.1073/pnas.2024792118

Wu, S., Lin, X., Bian, Z., Lipson, M., Lafortezza, R., Liu, Q., . . . Masson, V. (2024). Satellite observations reveal a decreasing albedo trend of global cities over the past 35 years. *Remote Sensing of Environment*, *303*, 114003.

Zanaga, D., Van De Kerchove, R., Daems, D., De Keersmaecker, W., Brockmann, C., Kirches, G., . . . Fritz, S. (2022). ESA WorldCover 10 m 2021 v200.

Zhao, L., Lee, X., & Schultz, N. M. (2017). A wedge strategy for mitigation of urban warming in future climate scenarios. *Atmospheric Chemistry and Physics*, *17*(14), 9067–9080.

Zhao, L., Lee, X., Smith, R. B., & Oleson, K. (2014). Strong contributions of local background climate to urban heat islands. *Nature*, *511*(7508), 216–219. doi: 10.1038/nature13462

Zhao, L., Oleson, K., Bou-Zeid, E., Krayenhoff, E. S., Bray, A., Zhu, Q., . . . Oppenheimer, M. (2021). Global multi-model projections of local urban climates. *Nature Climate Change*, *11*(2), 152–157.